Silicon (2020) 12:443–458
https://doi.org/10.1007/s12633-019-00151-3

ORIGINAL PAPER

Precise Description of the Variances of Electronic Bands in the $Si_{1-y}C_y$ Alloys Calculated with a Modified Becke-Johnson Exchange Potential

Mohamed Rahmani [1] · Abdelkader Yakoubi [1]

Received: 22 November 2018 / Accepted: 27 March 2019 / Published online: 5 April 2019

Abstract

In the present research paper, the structural, electronic and thermodynamic properties of the $Si_{1-y}C_y$ binary in a super cell consists of 08, 16 and 32 atoms were studied. The Full Potential-Linearized Augmented Plane Wave (FP-LAPW) method was used within the Density Functional Theory (DFT); which was performed directly in WIEN2K code.. The exchange and correlation potential is treated with the local density approximation (LDA). The deviation of lattice parameter was analyzed by the use of Vegard's Law depending on the concentration and, therefore, the results seem to obey the Vegard's law. Moreover, the modified exchange potential proposed by Becke -Johnson to calculate the gap were applied. The results achieved by the local density approximation (LDA) and potential of modified Becke -Johnson (MBJ-LDA) was discussed. Difference in the gap was observed especially in low concentrations y = 0.125; the gap value increases from −0.016 eV to 0.177 eV and when y = 0.5 the gap improved from 1.302 eV to 2.272 eV obtained by the LDA and the MBJ respectively; close to the experimental value 2.39 eV. Next, in order to study the microscopic origin of the bowing gap, Zunger's approach was introduced. Finally, thermodynamic properties were calculated as well as the results were discussed. Based on the results, it can be concluded that the values obtained are in a better agreement with those of other theoretical and experimental data.

Keywords Silicon carbide · Density functional theory · Local density approximation · Modified Becke-Johnson · Alloys · Electronic properties · Thermodynamic properties

1 Introduction

Silicon carbide (SiC) is one of the promising semiconductors regarding to its utility in technology and industrial applications of great frequency and high temperature [1–3]. Quite recently, considerable attention has been paid to Silicon carbide (SiC) because of its potential applications in nano-electronic devices [4–19], Solar cells [20],Visible-light [21], photocatalytic activity [21] and Ceramic foam materials [22].

For several years, great effort has been devoted to the study of binary alloy $Si_{1-y}C_y$, in order to correctly determine and understand its behavior, with several concentrations especially in the low concentration of C in the binary $Si_{1-y}C_y$ [23, 24] although, the results are neither satisfactory, nor that substantially close to the experimental outcomes.

Based on the findings in literature presented herein, the purpose of this paper is to look for responses that are consistent with the hypothesis that binary $Si_{1-y}C_y$ is metal in low concentration [25]. Work is carried out to study it's electronic properties by calculating the energy gap; the remarkable properties of the $Si_{1-y}C_y$ binary alloys which were ensured by employing the modified Becke–Johnson (mBJ) exchange potential [26–29].

In this paper, we reported the calculations of the structural and electronic properties of $Si_{1-y}C_y$ binary alloy with the use of supercells consists of 08, 16 and 32 atoms to understand thoroughly the effect of the cell sizes as well as the concentration of C in Si.

Further, we applied the full potential linearized augmented-plane-wave (FP-LAPW) method as the basis of density functional theory (DFT). In this approach, the local density approximation (LDA) and the composition dependence of the structural and electronic properties were used to identify parameter mesh and energy gap. In addition to this, we employed the modified Becke -Johnso method (mBJ) to analyze and compare the energy gaps.

✉ Mohamed Rahmani
rahmani_m77@yahoo.fr

[1] Laboratoire d'Étude des Matériaux & Instrumentations Optiques, Physics Department, University Djillali Liabes of Sidi Bel Abbes, Sidi Bel Abbes, Algeria

Table 1 Lattice parameter values, bulk modulus and its first pressure derivative obtained at equilibrium volume of C-Si and $Si_{1-y}C_y$ with 08 atoms super cell using both LDA and VCA compared to experimental and other theoretical works

Y	a(Angstrom) with LDA	a(Angstrom) with (VCA)	Other calculated in (Angstrom)	Exp. in (Angstrom)	B (Gpa)	B′
0	5.463	5.463	5.314[a]	5.429[b]	74.6654	4.5669
			5.4317[d]	5 .431[c]	99[b]	4.2[b]
			5.49[e]			
0.125	5.213	5.222	5.218[a]		106.8791	4.2288
0.25	4.979	4.981	4.979[a]		125.9035	4.2262
0.375	4.69	4.74	4.694[a]		162.2396	4.03
0.5	4.332	4.499	4.329[a]		229.0889	3.9694
0.625	4.201	4.258	4.202[a]		247.0565	3.9148
0.75	4.033	4.017	4.038[a]		280.897	3.862
0.875	3.816	3.776	3.821[a]		344.5318	3.8552
1	3.535	3.535	3.540[a]	3.567[b]	465.1424	3.6645
			3.533[d]			
			3.51[e]		443[b]	4.00[b]

[a] Réf. [10]
[b] Réf. [39]
[c] Réf. [40]
[d] Réf. [41]
[e] Réf. [42]

Table 2 Lattice parameter values, bulk modulus and its first pressure derivative obtained at equilibrium volume of C-Si and $Si_{1-y}C_y$ with 16 atoms super cell using both LDA and VCA compared to experimental and other theoretical works

Y	a(Angstrom) withLDA	a(Angstrom) with(VCA)	Other calculated in (Angstrom)	Exp. in (Angstrom)	B (Gpa)	B′
0	5.463	5.463		5 .431[c]	74.5105	4.583
					99[b]	4.2[b]
0.0625	5.375	5.3425			76.7292	4.4142
0.125	5.238	5.222	5.238[a]		103.503	4.2052
0.1875	5.154	5.1015			107.6236	4.1926
0.25	5.062	4.981	5.062[a]		113.3498	4.1039
0.3125	4.954	4.8605			121.3791	4.2505
0.375	4.663	4.74	4.663[a]		146.3698	3.9934
0.4375	4.775	4.6195			133.3805	4.1029
0.5	4.668	4.499	4.668[a]		148.5156	3.5729
0.5625	4.544	4.3785			161.3879	4.2828
0.625	4.41	4.258	4.410[a]		184.8151	3.696
0.6875	4.257	4.1375			211.8672	4.0611
0.75	4.138	4.017	4.138[a]		237.8094	4.9403
0.8125	4.005	3.8965			283.3831	4.5951
0.875	3.853	3.776	3.853[a]		335.609	4.4863
0.9375	3.681	3.6555			393.0672	3.9728
1	3.535	3.535		3.567[b]	350.5429	4.3776
					443[b]	4.00[b]

[a] Réf. [10]
[b] Réf. [39]
[c] Réf. [40]

Table 3 Lattice parameter values, bulk modulus and its first pressure derivative obtained at equilibrium volume of C-Si and $Si_{1-y}C_y$ with 32 atoms super cell using both LDA and VCA compared to experimental and other theoretical works

Y	a(Angstrom) with LDA	a(Angstrom) with (VCA)	Other calculated in (Angstrom)	Exp. in (Angstrom)	B (Gpa)	B′
0	5.402	5.402	–	5.429[a]-5.431[b]	95.9726	4.1615
					99[b]	4.2[b]
0.03125	5.357	5.34365625	–		97.614	4.2018
0.09375	5.263	5.22696875	–		103.2196	4.1835
0.5	4.333	4.4685	–		234.3279	4.4948
1	3.535	3.535	–	3.567[a]	307.9082	4.3257
					443[b]	4.00[b]

[a] Réf. [39]

[b] Réf. [40]

As a result of investigations, this paper aims to describe correctly the electronic properties such as band gap in accordance with the current calculations that we set forth to be used to model the electronic properties of semiconductors.

The main objective was, thus, to present a full potential linear augmented plane wave method within DFT to calculate structural properties and electronic band structure of the deviation of the lattice parameters, and to give some observations as regards the utilization of the gap relative to Vegard's law [30–33].

In this paper, we have compared the obtained results with the experimental and theoretical investigations. The remainder of the paper is organized as follows: Section II outlines the computational details, Section III discusses the structural, electronic and thermodynamic properties, Results are presented in Section IV, and finally, Section V concludes the paper.

2 Computational Details

To explore the structural, electronic and thermodynamic properties of $Si_{1-y}C_y$ binary alloy. We presented an application of the method of Full Potential Linearized Augmented-Plane-Wave (FP-LAPW) [34] that is implemented in WIEN2K code [35]. Next, we used two approximations to the potential exchange and correlation. The first; is the local density approximation (LDA) parameterized by Perdew and Wang in [36–38] and the second is the approximation of the modified potential exchange proposed by Becke-Johnson (mBJ) in [26–29].

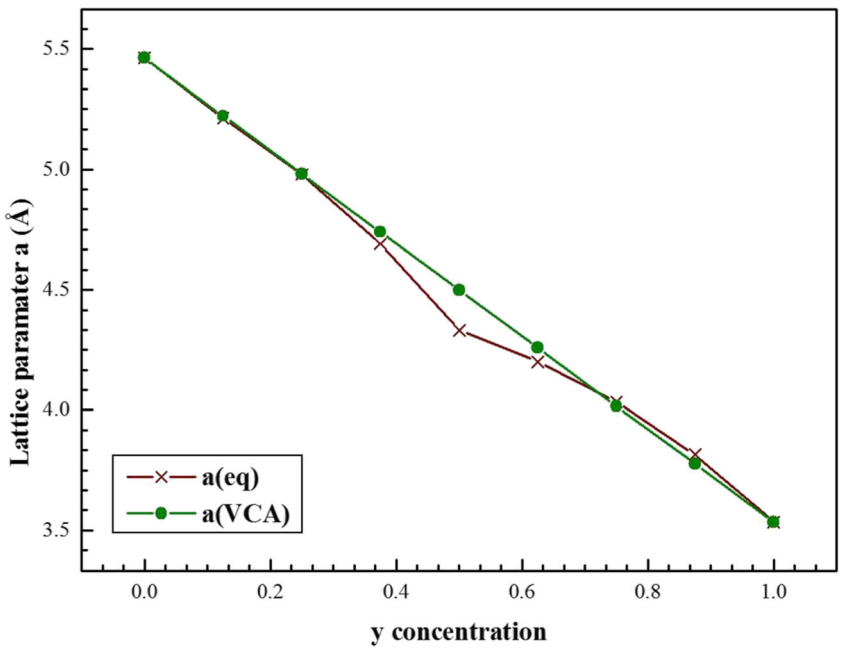

Fig. 1 Composition dependence of the calculated lattice constants of $Si_{1-y}C_y$ binary alloy compared with Vegard's Law

Table 4 The energy band gap of the $Si_{1-y}C_y$ binary alloy compared to experimental and other theoretical works

Atom(s)	E_g (eV) LDA Our work	E_g(eV)MBJ Our work	E_g(eV) VCA	Other calculated	Experimental data
Si	0.578 (−50.6%)	1.295 (+10.68%)	1.357	0.52[f]-1.75[d]	1.17[h]
C	4.763(−13.08%)	5.638 (+2.88%)	5.639	4.01[f]-5.9[d]	5.48[h]-5.5[e]
0[a]	0.591	1.301	1.342	1.05[e]	
0.125[a]	−0.35	0.177	0.24		
0.25[a]	0.012	0.307	0.309		
0.375[a]	0.712	1.478	1.084		
0.5[a]	1.302	2.272	2.354	1.31[e]-2.2[f]-4.3[d] 2.26[g]	2.39[d]
0.625[a]	1.521	2.233	2.172		
0.75[a]	1.472	2.298	3.322		
0.875[a]	2.963	3.822	3.854		
1[a]	4.763	5.635	5.366	4.88[d]	
0[b]	0.591	1.281			
0.0625[b]	0	0.357			
0.125[b]	0.034	0.425			
0.1875[b]	0.044	0.605	0.015		
0.25[b]	0.104	0.816			
0.3125[b]	0.186	0.933	0.229		
0[c]	0.644	1.062	1.272		
0.03125[c]	0.267	0.862	0.908		

[a, b, c] 8atoms, 16atoms supercell and 32 atoms respectively

[d] Ref. [25]

[e-h] Ref. [5]

[f] Ref. [44]

[g] Ref. [41]

In order to verify the validity of the proposed method, we carried out several experiments to find out two essential parameters, which are perfectly described the studied systems. The first parameter is the product of the muffin-tin medium R_{MT} ray and K_{MAX} vector ($R_{MT}\times K_{MAX}$, noted RK_{MAX}). The particular choice of muffin tin R_{MT} rays is performed so that the interstitial region between the different spheres is rendered as small as possible in order to ensure a rapid convergence. Indeed, small values of these rays involved a larger pore region. However, the latter is processed by planar waves, so that calculations time will be more important.

The second parameter is the number of special k-points that is used for integration in the Brillouin zone. In particular, we used the product $R_{MT}\times K_{MAX} = 7$ and the $R_{MT} = 1.9$ (a.u) and 1.8 (a.u) for the Si and C, respectively. Furthermore, the number of special k-points in the whole Brillouin zone (BZ) was selected as 200.

The optimization is based on the convergence of values related to the calculation's properties, The energy convergence that was chosen as 1mRy through eight iterations is necessary to achieve the convergence. The G_{MAX} setting = 12 $(a.u)^{-1}$ Basic functions (electronic densities, potential...) are extended in combinations of spherical harmonics around atomic sites with a cutoff $L_{MAX} = 10$ and in a series of Fourier in the pore region, The separation energy of valence and core states (cut-off energy) was chosen as −6 Ry. The electronic configuration of Si and C is as follows:

Si: [Ne] 3S23P2 and C: [He] 2S22P2. However, we have treated the States Si: [Ne] and C: [He] as the states of heart and the rest, that is to say, Si:3S23P2 and C:2S22P2 as the states of valence in our calculations.

3 Results and Discussion

3.1 Structural Properties

The properties of the fundamental state of $Si_{1-y}C_y$ binary alloy are obtained; applying a non-relativistic calculation by

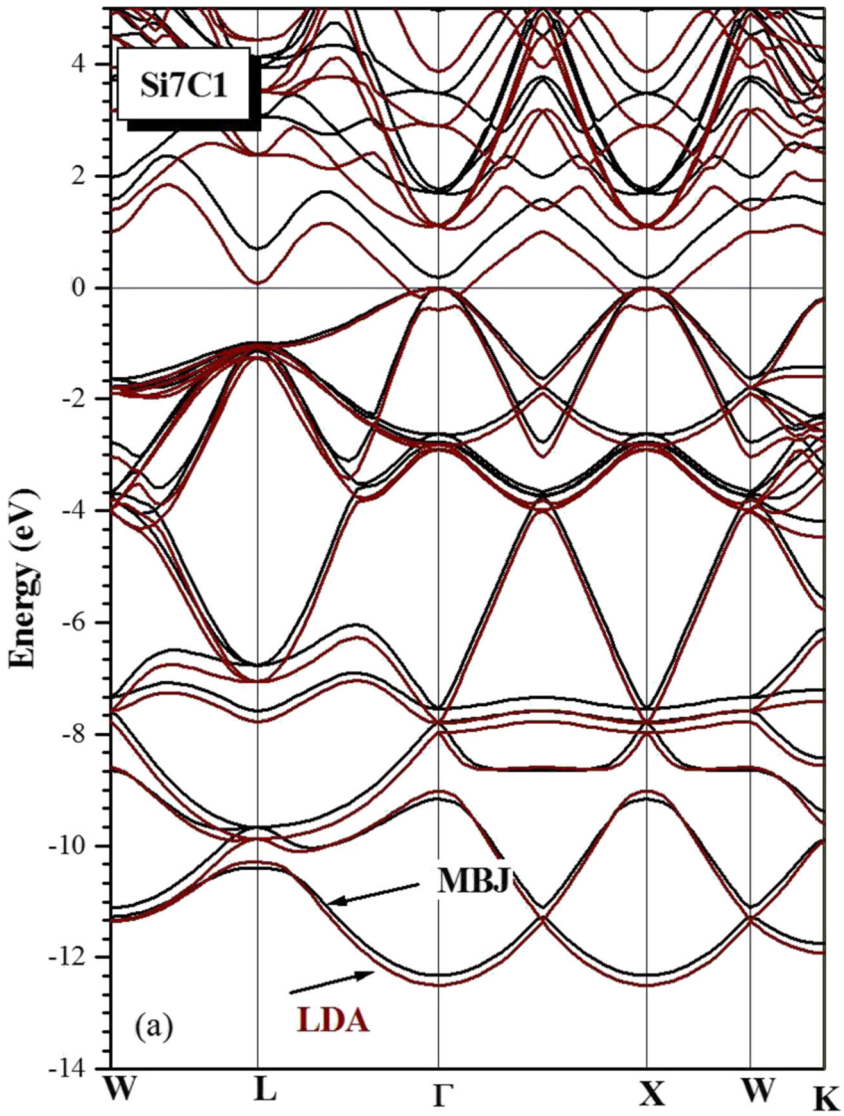

Fig. 2 **a:** The band structure for Si7C1 using LDA and mBJ-LDA calculation. **b:** The band structure for C using LDA and mBJ-LDA calculation. **c:** The band structure for Si using LDA and mBJ-LDA calculation

minimizing the total energy using the Murnaghan Equation Of State (EOS).

We first take the cubic crystal structure (diamond structure) and then derive the procedure. The main objective is to get the balance of the system. Once the balance is reached, we can calculate the structural properties. In this way, the calculation has been carried out for a supercell consists of 08, 16 and 32 atoms with a different concentration value of "y" for each supercell, equilibrium lattice parameters and bulk modulus B as well as its first derivative B', which are discussed and compared with other calculations data investigations as can be seen from in Tables 1, 2 and 3.

Moreover, it should be noted that the lattice parameters obtained by this calculation show a good agreement with the results found in the literature that were demonstrated by either; the experiments [39] or the other calculations.

It should also be noted that the lattice parameter "a" is inversely proportional to the component "y" in the $Si_{1-y}C_y$ binary alloy. (see Fig. 1).

To illustrate, a comparison was made using Vegard's law. This law is cosidered as an approach that gives deviations from the linearity of lattice Parameter curve. Where 'a' is the lattice constant which is assumed to be "a" as a function of the concentration "y", the lattice Parameter curve. Where 'a' is the lattice constant which is assumed to be binary alloy, the lattice parameter is written according to Vegard's law, in the case of binary alloy, as follows [30–33]:

$$a\left(A_{1-y}B_y\right) = (1-y)a_A + y a_B \quad (1)$$

Where a_A and a_B are the crystal parameters of the compounds A and B respectively; $a(A_{1-y}B_y)$ is the lattice parameter of their binary compound $A_{1-y}B_y$.

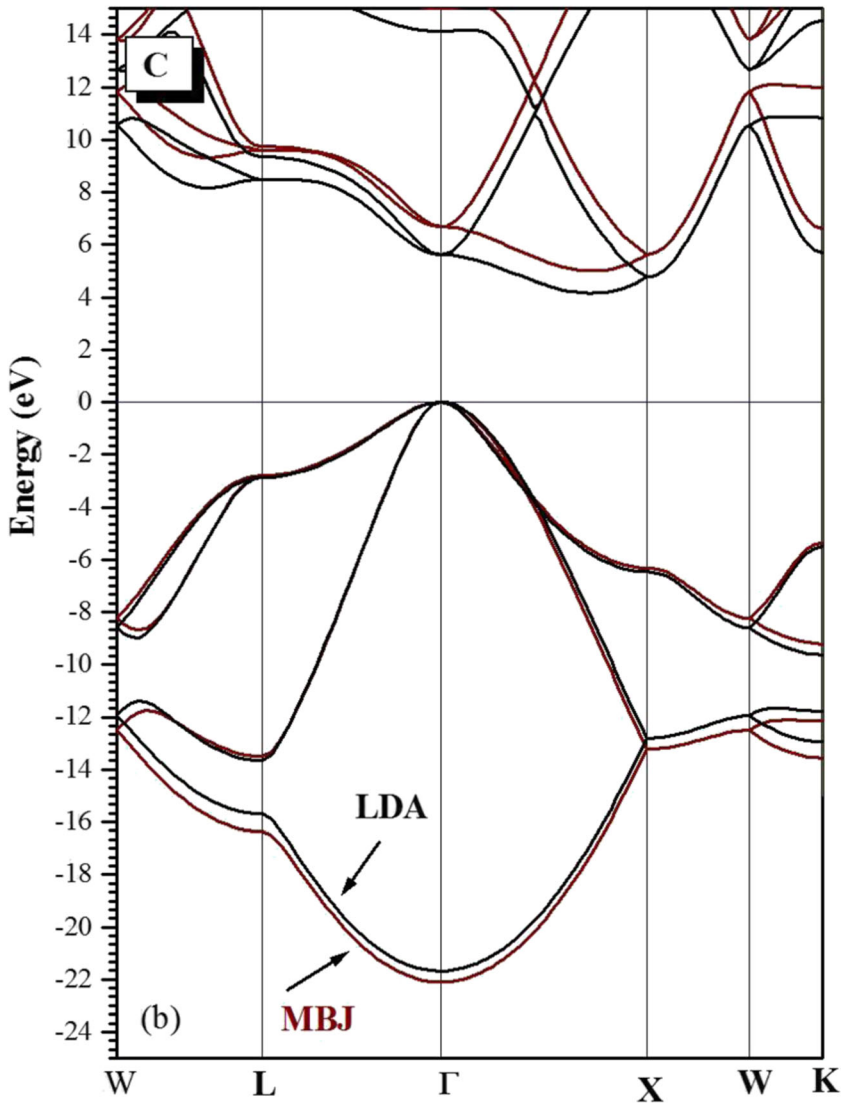

Fig. 2 (continued)

We can observe that there is a small deviation between the lattice parameter calculated by the LDA and that of Vegard's Law, with a difference ranged between - 0.002 and 0.04 and between −0.07 and 0.16 in the calculations of 8-atoms supercell and 16-atoms supercell, respectively.

It is interesting to note that a smaller size of C atoms incorporated into the lattice of $Si_{1-y}C_y$ binary reduces the average volume of the alloy and hence, it's not difficult to demonstrate that our binary alloy is in a very good agreement with Vegard's Law in terms of the stated values.

Additionally, the modulus of rigidity and its derivatives is proportional to "y" concentration of the carbon in the binary alloy. Accordingly, this also indicates that by giving a rigidity and stability to this binary compound, it is possible therefore to note that its value is important.

3.2 Electronic Properties

In this section, we explore the possibility of studying the electronic properties of $Si_{1-y}C_y$ binary alloy by highlighting the importance of energy gaps for optimizing and expanding the applications of semiconductor devices.

The energy gap is known to be one of the most important parameters because it is strongly connected to their wavelength of operation in optoelectronic applications. The bands structures were calculated according to the directions of high symmetry in the Brillouin zone of a cubic mesh, and the calculation of the lattice parameters with optimization. Further, the approach of Vegard's law and the approximation of mBJ also has been used in a view of improving the results of the energy gaps. Accordingly, the silicon and the carbon as well as

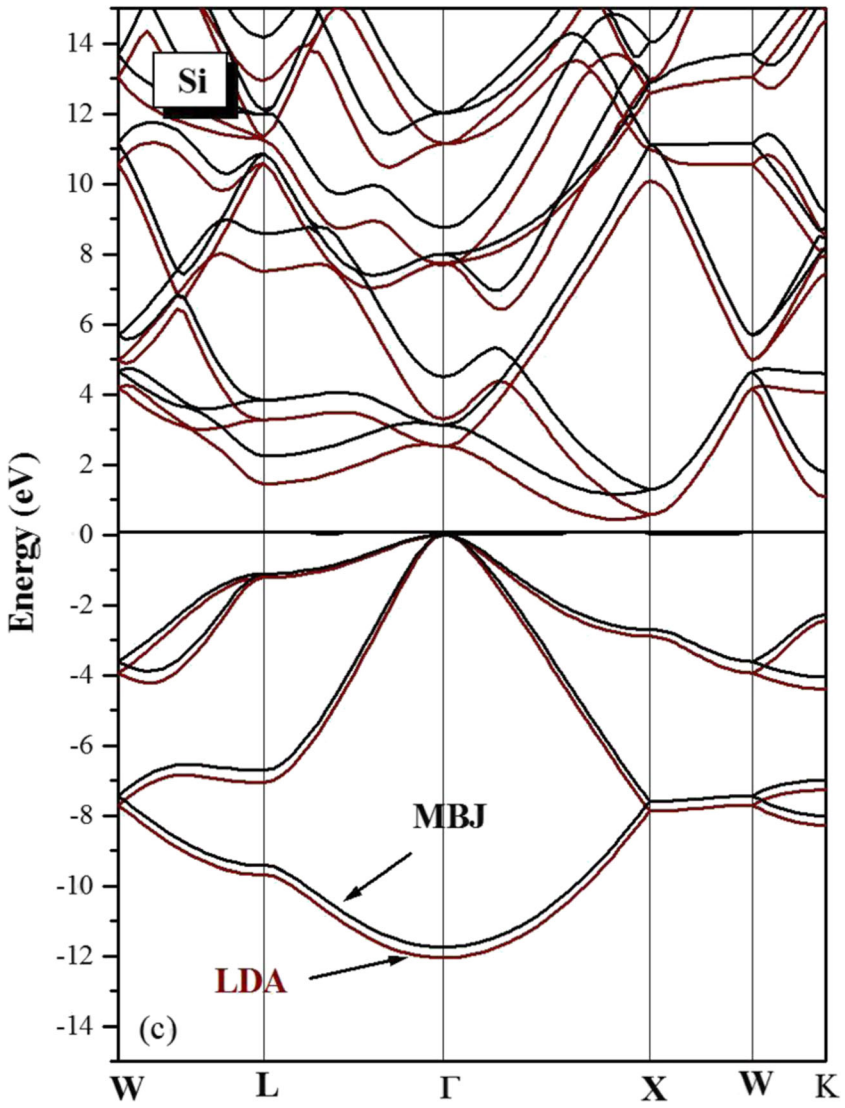

Fig. 2 (continued)

their binary silicon carbide compound are indirect gap semiconductors and thus, it has been concluded that the $Si_{1-y}C_y$ binary alloy also has an indirect gap, in the direction $\Gamma \rightarrow X$.

The band structures are calculated using two approximations LDA and mBJ-LDA, the results obtained for the $Si_{1-y}C_y$ binary alloy and their constituents Si and C are depicted in Table 4.

As can be seen from Fig. 2 (a), (b) and (c)., there is a displacement with energy spacing in the conduction band. In contrast, the gap value increases from −0.016 eV to 0.177 eV for the concentration y = 0.125 or (12.5%). The results are compared with experimental and theoretical data available in the literature [5, 25, 41, 44]. The results thus obtained, by the use of the LDA, are underestimate what is predicted and expected compared to the experience, given the fact that the DFT-based methods adopt this behavior.

Anticipatively, the gap values calculated using the LDA 1.302 eV are underestimated and incomparable with those of the experiment 2.39 eV for y = 0.5 concentration or (50%). By contrast, in using the mBJ approximation, the gaps are significantly improved 2.272 eV; they are closer to those of the experiment. In fact, the mBJ approximation allows us to calculate the energy gaps with a precision which overcomes the problem of the failure of DFT on the gap [41], that has been demonstrated in our results.

Figure 3 shows the variation of the energy gaps of the $Si_{1-y}C_y$ binary alloy in function of the concentration of "y".

Based on the above results, we should note that the energy gap does not increases linearly with concentration. The curves hence correspond to the quadratic interpolation (Fit) of the following form:

$$E(y) = E_0 + A\,y + B\,y^2 \quad (2)$$

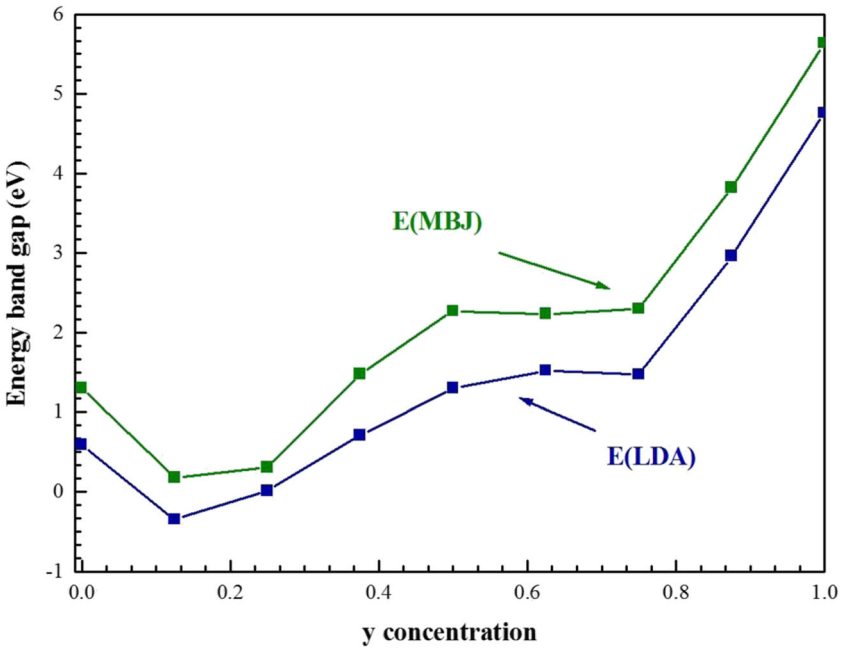

Fig. 3 Band gap energies of $Si_{1-y}C_y$ binary alloy as a function of C concentration using LDA and mBJ-LDA calculation

Where B is the disorder parameter of the energy gap, the results obtained are according to the approximations used:

$$\mathrm{LDA} : \mathrm{E(y)} = 0.62\text{–}2.97\, y + 6.73\, y^2 \quad (3)$$

$$\mathrm{mBJ} : \mathrm{E(y)} = 0.90\text{–}2.02\ \mathrm{y} + 6.43\ \mathrm{y}^2 \quad (4)$$

$$\mathrm{VCA} : \mathrm{E(y)} = 0.80\text{–}1.34\ \mathrm{y} + 5.88\ \mathrm{y}^2 \quad (5)$$

Consider Fig. 4 which depicts the band gap energies of $Si_{1-y}C_y$ binary alloy in function of C concentration obtained by the fit.

As follows from the figures shown above, it has been revealed that the bowing parameter is mainly due to differences between the length of lattice parameters and the factors of iconicity of the parents of the alloy compounds [45–47].

To understand and explain the physical origins of the bowing parameter we have adopted the approach of Zunger and al [48]. In this approach, the disorder parameter "*b*" is broken down into three different contributions. The deformation of the volume "b_{VD}", the charge transfer

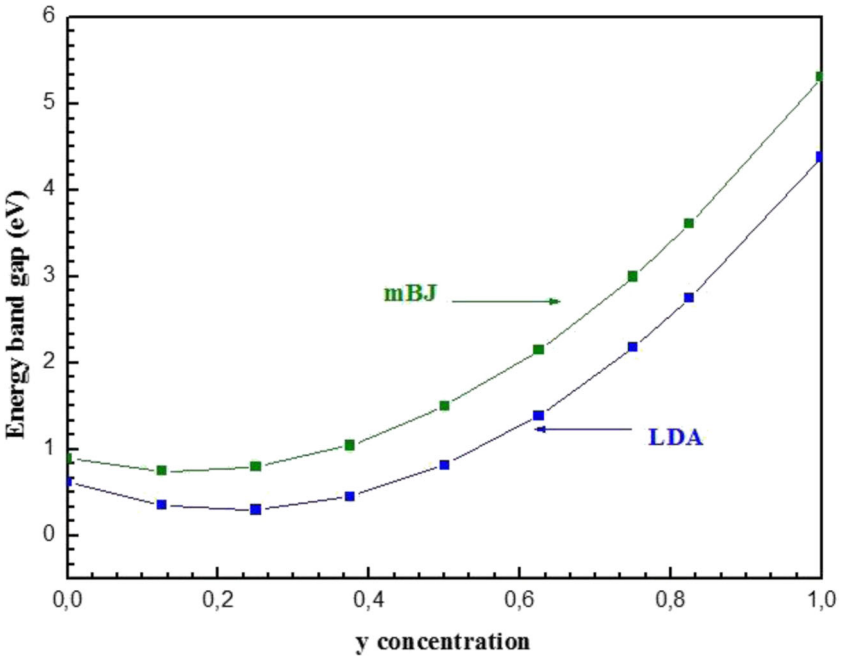

Fig. 4 Band gap energies of $Si_{1-y}C_y$ binary alloy in function of C concentration obtained by the fit

Table 5 Decomposition of optical bowing into volume deformation (vd), charge exchange (ce) and structural relaxation (sr) contributions

Y	Bvd(eV)	Bce(eV)	Bsr(eV)	B(eV)
0				
0.125	2.105	41.101	−0.999	42.207
0.25	1.021	21.399	0.006	22.426
0.375	0.651	12.843	−0.656	12.838
0.5	0.456	8.708	0.082	9.246
0.625	0.321	4.924	−0.036	5.208
0.75	0.194	10.308	0.341	10.844
0.875	−0.020	−37.087	0.004	−37.103
1				

"b_{CE}" and the structural relaxation "b_{SR}". Considering the fact that the dependence of the disorder parameter (the bowing) on the composition which is marginal, the authors have limited their calculations to the concentration y = 0.5. The overall coefficient of disorder parameter from y = 0.5 measure change of the gap, according to the following form:

$$\mathrm{AB}\ (a_{AB}) + \mathrm{AC}\ (a_{AC}) \rightarrow \mathrm{AB_{0.5}C_{0.5}}\left(a_{eq}\right) \tag{6}$$

a_{AB} and a_{AC} are the lattice parameters of the parent compounds Si and C, respectively; a_{eq} is the equilibrium lattice constant of the alloy. The reaction (06) is therefore broken down into three steps yields to:

$$\mathrm{AB}\ (a_{AB}) + \mathrm{AC}\ (a_{AC}) \overset{VD}{\rightarrow} \mathrm{AB}\ (a) + \mathrm{AC}\ (a) \tag{7}$$

$$\mathrm{AB}\ (a) + \mathrm{AC}\ (a) \overset{CE}{\rightarrow} \mathrm{AB_{0.5}C_{0.5}}(a) \tag{8}$$

$$\mathrm{AB_{0.5}C_{0.5}}(a) \overset{SR}{\rightarrow} \mathrm{AB_{0.5}C_{0.5}}\left(a_{eq}\right) \tag{9}$$

To simplify, the first step measures the effect of the volume deformation (vd) on the disorder parameter. The corresponding contribution b_{VD} represents the relative response of the band structure of binary compounds AB and AC to the hydrostatic pressure, which in this case it approaches from the change in their settings related to the individual equilibrium lattice constants to the alloy value $a = a(y)$ (Vegard's law).

Else, the second contribution is that of the charge exchange (ce). The b_{CE} contribution reflects the effect of the charge transfer that is due to the behavior at the lattice constant a. Moreover, the last phase measures the changes due to the structural relaxation (sr), in passing from the unrelaxed to the relaxed alloy by b_{SR} and therefore, the total parameter of disorder b (bowing) is defined as follows:

$$b = b_{VD} + b_{CE} + b_{SR} \tag{10}$$

$$b_{VD} = 2[\ \varepsilon_{\mathrm{AB}}(a_{AB}) - \varepsilon_{\mathrm{AB}}(a) + \varepsilon_{\mathrm{AC}}(a_{AC}) - \varepsilon_{\mathrm{AC}}(a)] \tag{11}$$

$$b_{CE} = 2[\ \varepsilon_{\mathrm{AB}}(a) + \varepsilon_{\mathrm{AC}}(a) - 2\varepsilon_{\mathrm{ABC}}(a)] \tag{12}$$

$$b_{SR} = 4\left[\ \varepsilon_{\mathrm{ABC}}(a) - \varepsilon_{\mathrm{ABC}}\left(a_{eq}\right)\right] \tag{13}$$

>Where "ε"is the calculated energy gap for the lattice parameters and the atomic structures indicated, the all terms of the Eqs. (11, 12 and 13) are determined by a calculation of auto-coherent of band structure for the two approximations LDA and mBJ. The results thus obtained for these different contributions the values of the total gap bowing are figured out in Table 5.

By applying the Zunger's approach [48]; we can reveal that the main contribution to the total gap bowing of $Si_{1-y}C_y$ binary alloy is owing to the charge exchange effect and

Table 6 Selection of thermal properties at 300 K: C_v and C_p in J/mol K; Debye temperature (K)

Elements	C_v(J/mol K) (at room temperature)	Cp(J/mol K) (at room temperature)	Θ_D (K) (at room temperature)	Θ_D (K) (at base temperature)	Θ_D (K) (at high temperature)
Si	1.96	1.98	670.49 645[a]	673.96	660.36
C	6.84	6.85	1823.49 1860[b]	1824.50	1762.78
Si_7C_1	1.60	1.63	631.56	638.50	604.21
Si_6C_2	1.54	1.57	699.85	706.61	674.17
Si_5C_3	1.42	1.44	804.00	809.56	764.35
Si_4C_4	1.25	1.27	964.34	969.07	913.48
Si_3C_5	1.18	1.20	1039.55	1044.24	980.03
Si_2C_6	1.06	1.07	1151.92	1155.97	1083.18
Si_1C_7	9.22	9.29	1325.67	1329.31	1240.24

[a] Ref. [56]

[b] Ref. [57]

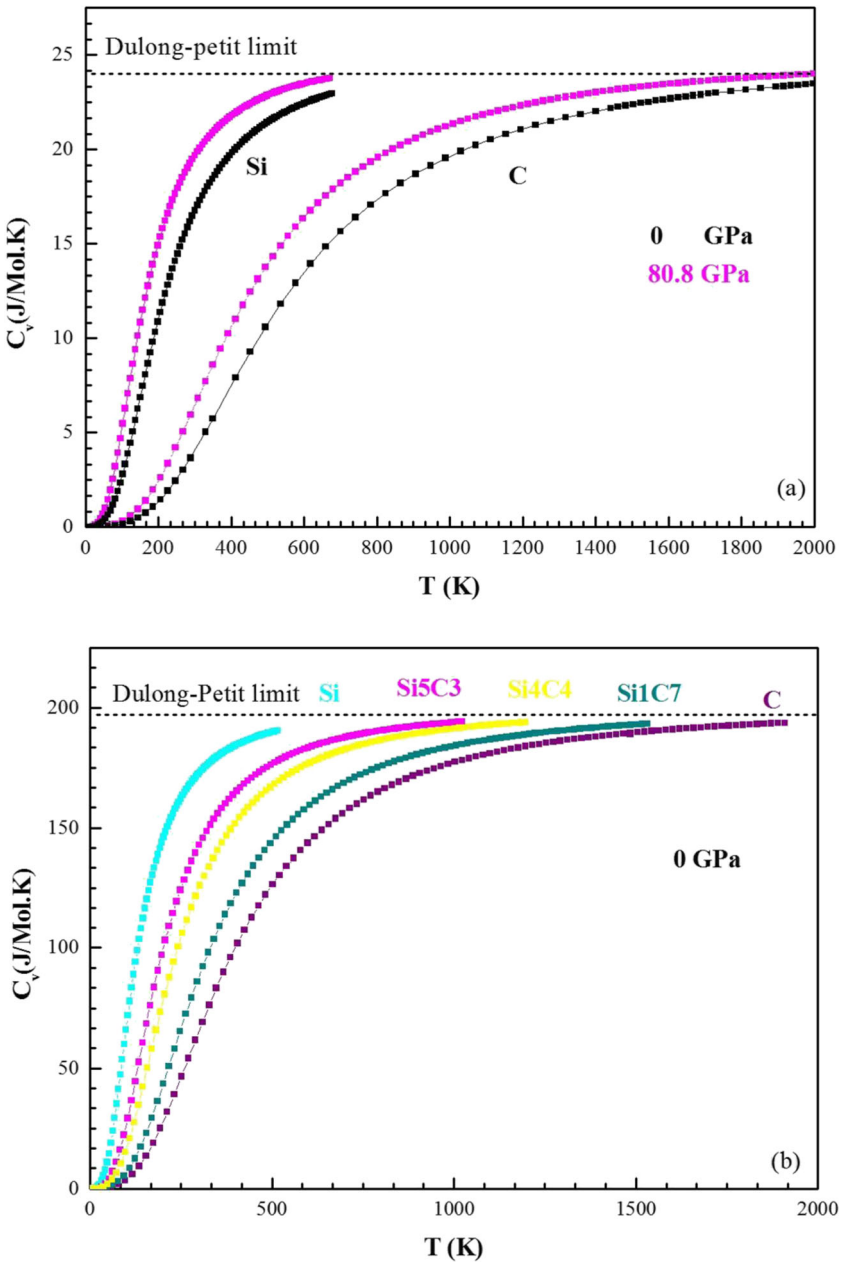

Fig. 5 **a:** Heat capacity at constant-volume of Si and C with temperature, at the 0–80 GPa pressure range. **b:** Heat capacity of the the binary alloy $Si_{1-y}C_y$ with the temperature

the difference in electronegativity of the atoms Si (1.9) and C (2.55). Notwithstanding the fact that the contribution of the term of deformation of volume b_{VD} is low, it remains remarkable because of the difference between the lattice parameters of the parent compounds Si and C.

Particularly, we may conclude that the term b_{SR} is low because we have considered that the alloy $Si_{1-y}C_y$ is ordered/in order. The disorder parameter of the alloy $Si_{1-y}C_y$ is more larger in the lower concentrations and gradually decreases as the value of "y" increases. Comparing the gap of the $Si_{1-y}C_y$ alloy there is a decrease of the pure Si gap by the addition of C in the low concentrations ($y < 0.25$). Indeed, this observation has been proved by other researches [25, 49].

Furthermore, we notice that the gap increases with C content. We interpreted as a matter of fact that the widening (the energy introduced by alloy disorder) is as a result of differences in ionic potentials between Si and C. The local distortion of the C atoms from the diamond lattice sites (about 0.14 A rms), and the statistical effects that leading to an inhomogeneous broadening of the interband transitions, as research shows in [47].

3.3 Thermodynamic Properties

In this work, we review the thermals properties of the C, Si and their binary alloys $Si_{1-y}C_y$. In effect, we used the computational package realized in the form of GIBBS [50]program which is based on the quasiharmonic Debye model [51].In addition to this, the determination of the thermodynamic properties is based on the knowledge of the thermal equation of state (EOS) and the chemical potential G(P,T) by by generating the GIBBS eq. G*(V, P, T):

$$G^*(V,P,T) = E(V) + PV + A_{vib}[\Theta(V),T] \quad (14)$$

This energy is solely in function of the volume, pressure and temperature only (V, P and T). According to the Debye model of the state density of phonon (vibration), the contribution A_{vib} is as follows:

$$A_{vib}(\Theta,T) = nKT\left[\frac{9}{8}\frac{\Theta}{T} + 3\ln\left(1-e^{\frac{-\Theta}{T}}\right) - D\frac{\Theta}{T}\right] \quad (15)$$

Where:

Θ Is the Debye temperature, n is the number of atoms per unit volume

$\frac{\Theta}{T}$ Represents the Debye integral for the isotropic solid

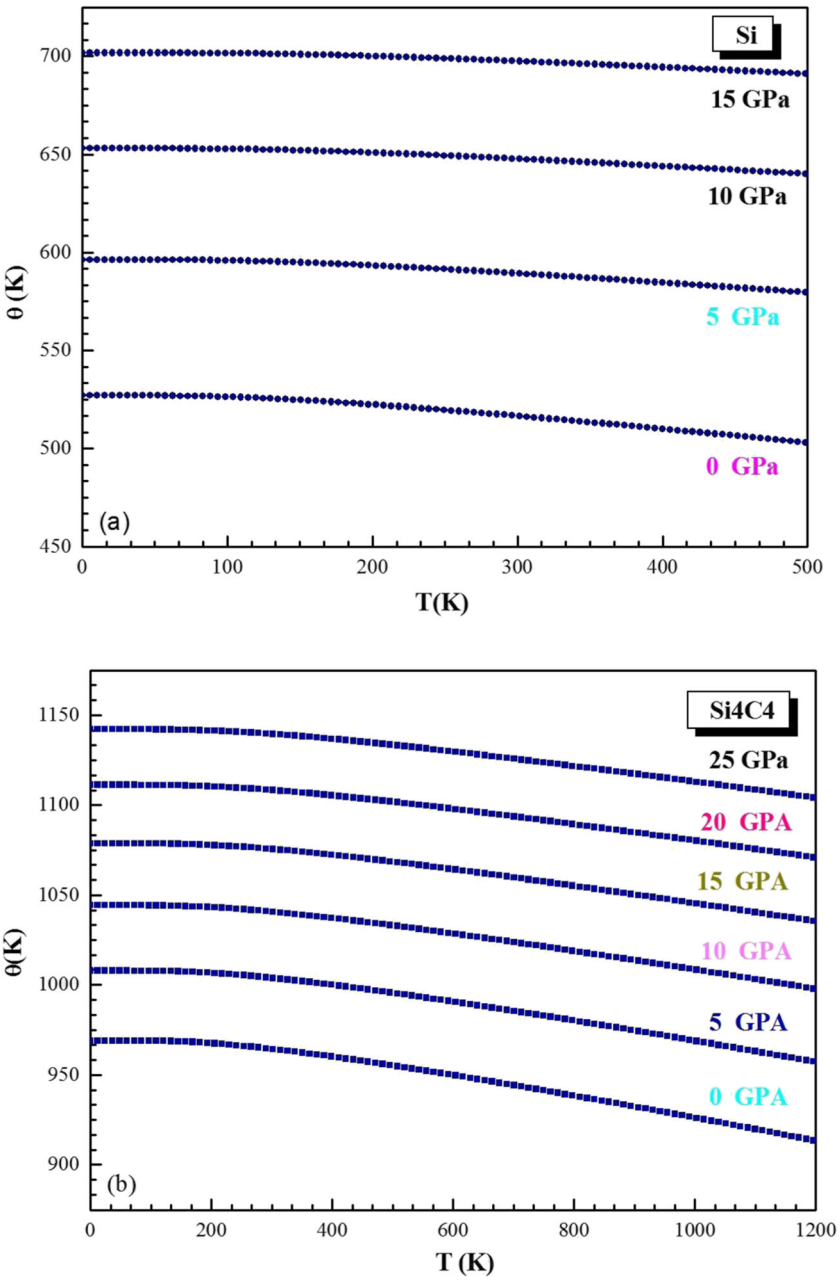

Fig. 6 **a:** The variation of Debye temperature with temperature for Si at 0–15 GPa. **b:** The variation of Debye temperature with temperature for Si4C4 at 0–25 GPa. **c:** The variation of Debye temperature with temperature for Si7C1 at 0–15 GPa**. d:** The variation of Debye temperature with temperature for C at 0–80 GPa

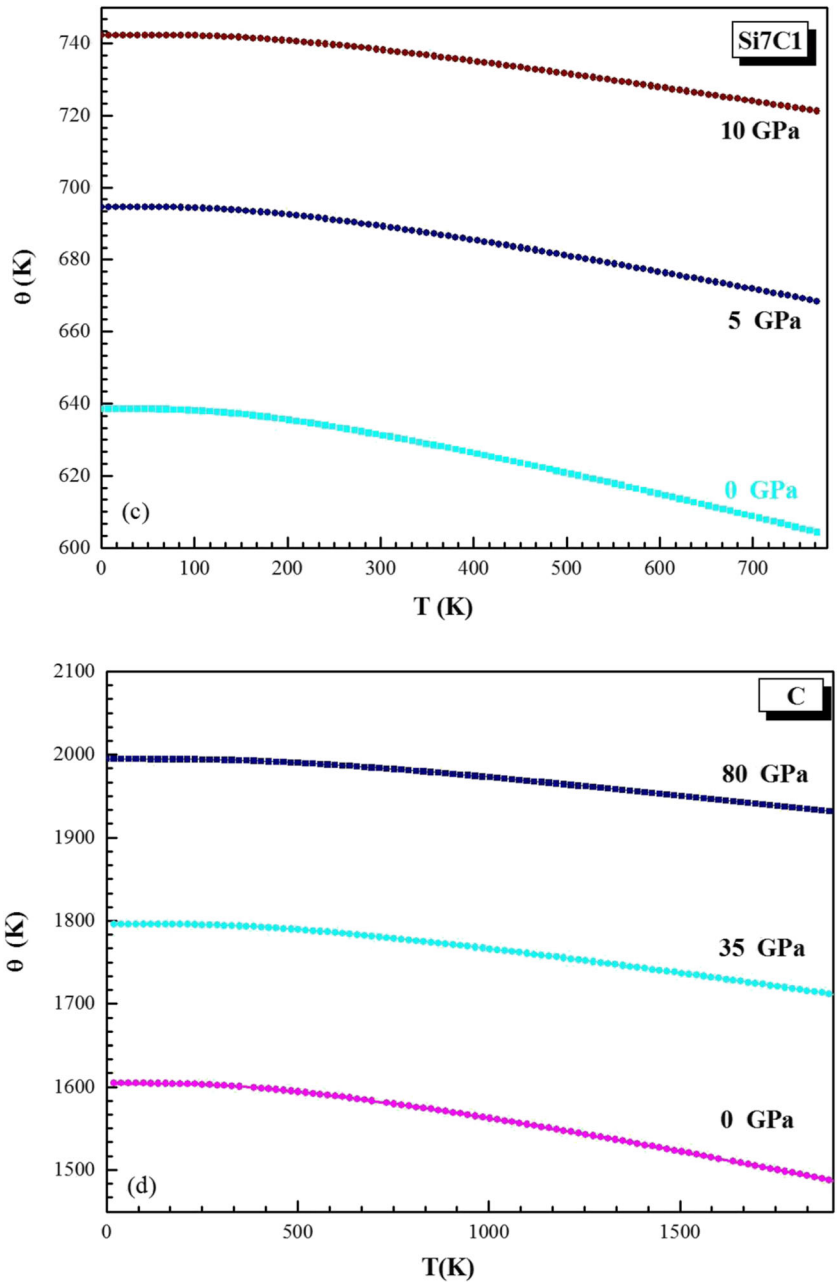

Fig. 6 (continued)

$$\Theta D = \frac{h}{K}\left(6\pi^2 V^{\frac{1}{2}} r\right)^{\frac{1}{3}} \sqrt{\frac{B_S}{M}} f(\sigma) \tag{16}$$

Where:

M is the molecular weight per unit volume
B_S is the module of the compressibility [52]:

$$B_S \cong B(V) = V \frac{d^2 E(V)}{d V^2} \tag{17}$$

$f(\sigma)$ is given by the following function [53, 54]:

$$f(\sigma) = \left\{3\left[2\left(\frac{2}{3}\frac{1+\sigma^{\frac{3}{2}}}{1-2\sigma} + \left(\frac{1}{3}\frac{1+\sigma}{1-\sigma}\right)^{\frac{3}{2}}\right]^{-1}\right\}^{\frac{1}{3}} \tag{18}$$

We obtain the pressure and temperature equilibrium by the minimization of the GIBBS function:

$$\left[\frac{\partial G^*(V,P,T)}{\partial V}\right]_{P,T} = 0 \tag{19}$$

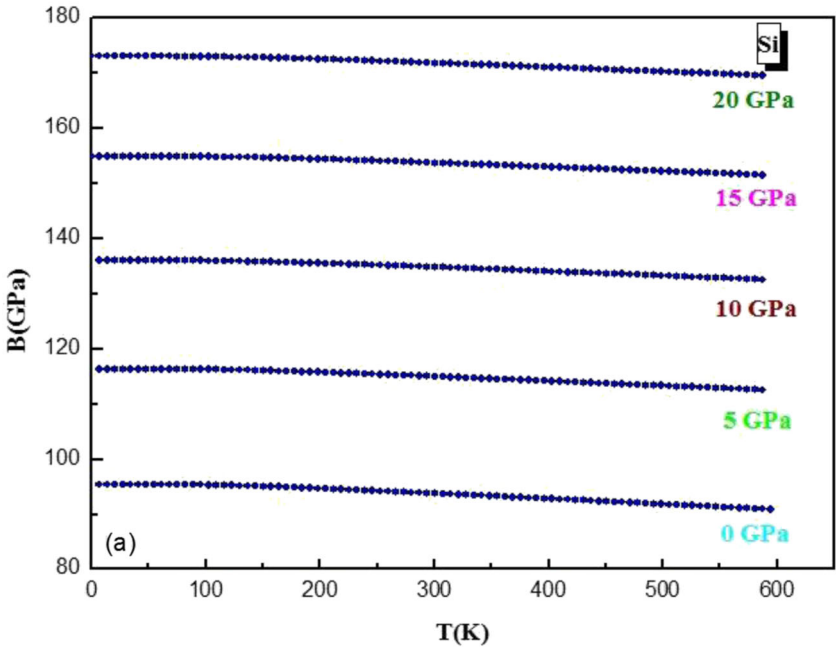

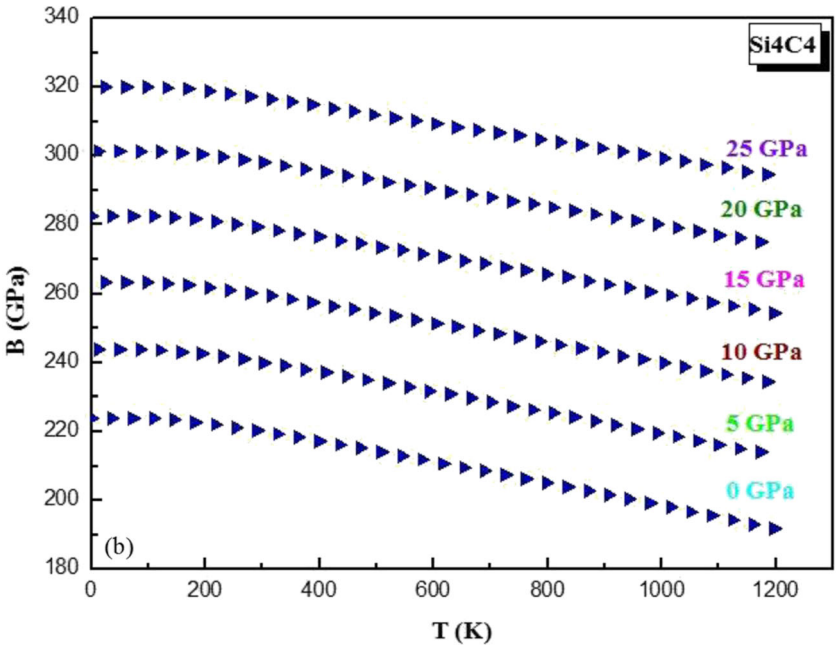

Fig. 7 **a:** The variation of the bulk modulus with temperature for Si at 0–20 GPa. **b:** The variation of the bulk modulus with temperature for Si_4C_4 at 0–25 GPa. **c:** The variation of the bulk modulus with temperature for Si_7C_1 at 0–10 GPa. **d:** The variation of the bulk modulus with temperature for C at 0–20 GPa

By resolution of the eq. (14) we can get specific heat at constant volume, Cv [55]:

$$Cv = 3nk\left[4D\left(\frac{\Theta}{T}\right) - \frac{3\,{}^{\Theta}/_{T}}{e^{\Theta/T}-1}\right] \tag{20}$$

Consider Table 6 below, which depicts the thermal properties results obtained at different room temperatures.

3.3.1 The Specific Heat at Constant Volume

At a very low temperature the expansion is negligible, the curve starts with a zero slope, then increases sharply from 50 to 500 K for Si; and from 100 to 1500 for C, and above 500 K for Si and 1500 for C. Also, the specific heat at constant volume C_v gets the linear regime.(see Fig. 5 (a)).

Otherwise, the Carbon has already a heat capacity of 15 J/mol K at 300 K and the Silicon does not reach a value of

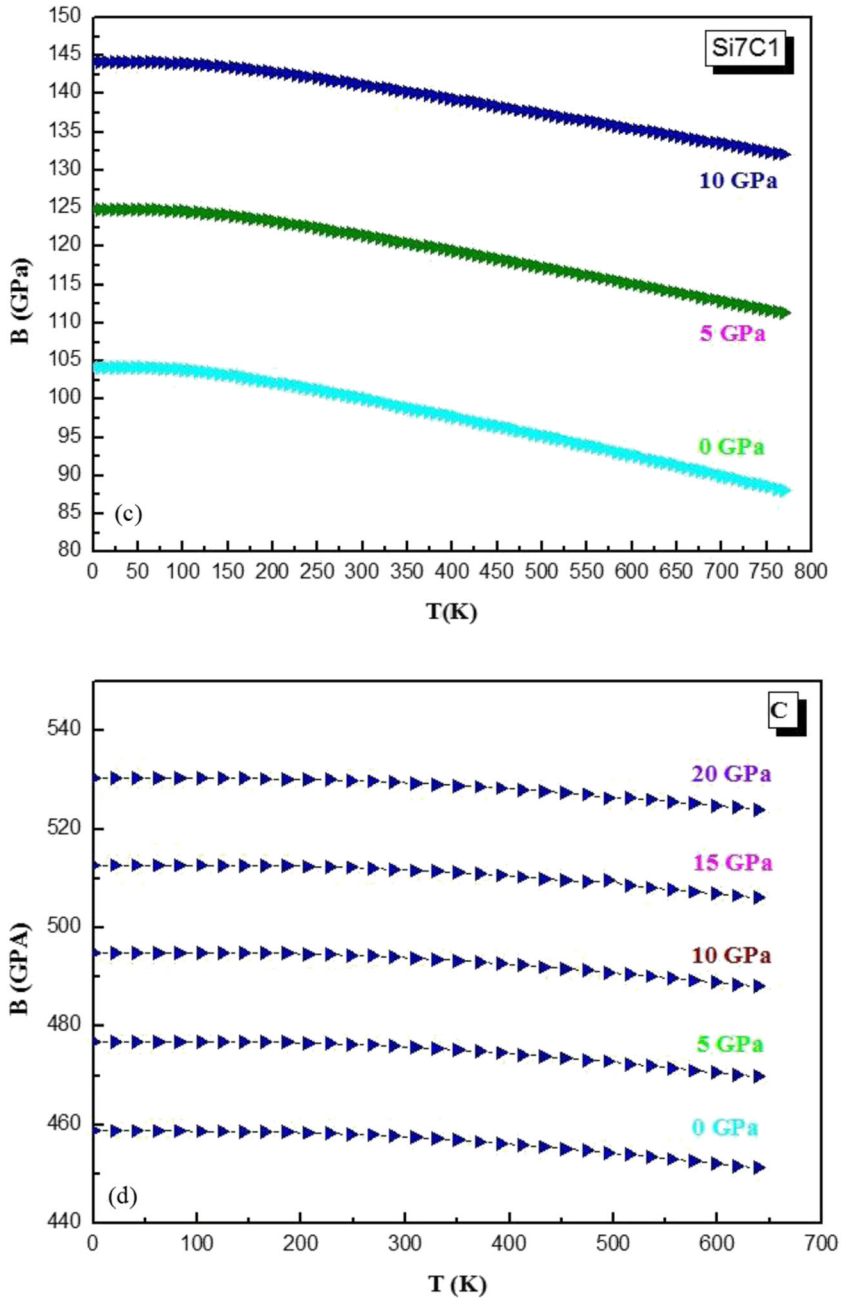

Fig. 7 (continued)

700 K, when the temperature is much greater than the Debye temperature. Therefore, the heat capacity at constant volume is thrice the value of the perfect gas at constant volume C_V and as such it is, it is the classical limit of Dulong-petit law (C_v (T) ≅ 3R);(See Fig. 5 (b)). The results obtained for the compounds Si and C are very close to the results found in the literature [56]. For binary $Si_{1-y}C_y$ the field of change is maintained between the heat capacity C_v of Si and the C_v of C as shown in Figs. 5(a) and 5(b).

3.3.2 Debye Temperature

The variation of Debye temperature ($\Theta_{D)}$ as a function of temperature and pressure for Si, C and $Si_{1-y}C_y$ binary alloy (y = 0, 1, 0.125, 0.5) was illustrated in Fig. 6 (a), (b), (c) and (d).

As can be seen from these figures, the general behavior of Θ_D under temperature and pressure for Si_4C_4 and Si_7C_1 does not differ from that of both these compounds; namely, Si and C.

For different pressure values, we notice that the Debye temperature is almost constant between 0 and 150 K and between 0 and 500 k for Si and C, respectively.

Additionally, it decreases linearly when temperature exceeds 200 K for Si and 600 k for C.

For y = 0.125 and y = 0.5 concentration, we reveal that the value of Debye temperature increases with the concentration. Substantially, the increase in pressure significantly affects the rate of change of Θ_D in temperature.

3.3.3 The Bulk Modulus

The discussed thermal properties are determined in temperature range from 0 to 600–650–800-1200 K for Si;C;Si_7C_1 and Si_4C_4 respectively. In the Fig. 7 (a), (b), (c) and (d), we represent the variation as a function of temperature and pressure at 0–25 GPa on bulk modulus *B* of Si, Si_4C_4, Si_7C_1, and C respectively.

The first remark that can be drawn from these figures is that the bulk modulus displays the same behavior under temperature and pressure for the compounds Si, C, Si_4C_4, and Si_7C_1. Therefore, the bilk modulus is inversely proportional to the temperature under different pressures range from 0 to 25 GPa. At a low temperature, the change in the value of *B* is very small, at finite temperature intervals below 100 K, 200 K, 150 K and 250 K for Si, C, Si7C1 and Si4C4; respectively.

Contrastingly, the decay of the value of *B* becomes more and more important for T ≥ 500 K at the high temperatures.

The results indicate that *B* values decreases with temperature at a given pressure and increases with pressure at a given temperature. As expected, the alloys become more compressible with the rising temperatures.

4 Conclusions

In this study, we have developed an approximate ab initio FP-LAPW method to investigate the structural and electronic properties of the Si; C and $Si_{1-y}C_y$ layer by the use of LDA and mBJ-LDA approximations. The band gap energies obtained from the calculated band structures are well agreed with the reported experimental data. For the concentration y = 0.5 and we obtained a gap of 2.272 eV, whereas for the low concentration y = 0.125 we have a prediction of the gap at 0.177 eV. In addition, we have also determined the origin of the energy gap with Zunger's approach; we have performed the microscopic atomic structure of the alloys.

Our work was completed by a thermodynamic study through the variation of the heat capacity at constant volume. The variations of Debye temperature and bulk modulus as well as the alloy interest thermal properties are also calculated using the quasi-harmonic Debye model.

Summing up the results, it can be concluded that $Si_{1-y}C_y$ layer has a very low energy and a large band gap and therefore, the alloy depends on the band of Si and C components.

This research was concerned with the $Si_{1-y}C_y$ that is very stable at high temperature. However, our results have great potential for other applications in hard conditions. The findings suggest that this material should be studied further for possible new electronic applications, and for all other semiconductor systems. Clearly, further research on the issue would be of interest.

Acknowledgements The authors would like to acknowledge the assistance of Dr. BENZERGA Noureddine (benznourijones@gmail.com) from the University of Djillali Liabes faculty of letters and arts in reviewing the paper. The authors would like also to acknowledge the valuable proofreading of M[e] OUENNAS Sara in the presence of TRANS-OFFICE (E-mail: transoffice2@gmail.com) which have improved the quality of this paper.

References

1. Pinaud F, Michalet X, Bentolila LA, Tsay JM, Doose S, Li JJ, Iyer G, Weiss S (2006) Advances in fluorescence imaging with quantum dot bio-probes. Biomaterials 27:1679–1687
2. Camassel J, Contreras S (2012) Matériaux semiconducteurs à grand gap: le carbure de silicium (SiC). *Techniques de l'ingénieur* 1990: 1–17
3. She X, Huang AQ, Lucía Ó, Ozpineci B (2017) Review of silicon carbide power devices and their applications. IEEE Trans Ind Electron 64:8193–8205
4. Bhatnagar, M.; Baliga, B. J.(03/1993) Comparison of 6H-SiC, 3C-SiC, and Si for power devices.IEEE Transactions on Electron Devices, vol. 40, issue 3, pp. 645-655
5. Rohlfing M, Krüger P, Pollmann J (1993) Quasiparticle band-structure calculations for C, Si, Ge, GaAs, and SiC using Gaussian-orbital basis sets. Phys Rev B 48:17791
6. Brunner K, Winter W, Eberl K, Jin-Phillipp N, Phillipp F (1997) Fabrication and band alignment of pseudomorphic Si 1− y C y, Si 1 − x− y Ge x C y and coupled Si1− yCySi1− x− yGexCy quantum well structures on Si substrates. J Cryst Growth 175:451–458
7. Theodorou G, Tsegas G, Kaxiras E (1999) Theory of electronic and optical properties of 3C-SiC. J Appl Phys 85:2179–2184
8. Itoh T, Hasegawa Y, Fujiwara T, Masuda A, Nonomura S (2004) Preparation of wide gap and low resistive hetero-structured SiC X films as wide gap window of solar cells. J Non-Cryst Solids 338: 123–126
9. Schmidt M, Schoepke A, Korte L, Milch O, Fuhs W (2004) Density distribution of gap states in extremely thin a-Si: H layers on crystalline silicon wafers. J Non-Cryst Solids 338:211–214
10. Yakoubi A, Bouhafs B, Ferhat M, Ruterana P (2005) Predictive study of electronic properties of silicon–carbon alloys. Mater Sci Eng B 122:145–151
11. Berger C, Song Z, Li X, Wu X, Brown N, Naud C, Mayou D, Li T, Hass J, Marchenkov AN (2006) Electronic confinement and coherence in patterned epitaxial graphene. Science 312:1191–1196
12. Ray AK, Huda M (2006) Silicon-carbide nano-clusters: a pathway to future nano-electronics. J Comput Theor Nanosci 3:315–341
13. Mélinon P, Masenelli B, Tournus F, Perez A (2007) Playing with carbon and silicon at the nanoscale. Nat Mater 6:479–490
14. Choyke WJ, Matsunami H, Pensl G (2013) Silicon carbide: recent major advances. Springer Science & Business Media

15. Merzkirch M, Blümel C, Rössler R, Schell K, Bucharsky E, Weidenmann K (2014) Manufacturing and characterization of interpenetrating SiC lightweight composites. Procedia CIRP 18:102–107
16. Román-Manso B, Vega-Díaz SM, Morelos-Gómez A, Terrones M, Miranzo P, Belmonte M (2014) Aligned carbon nanotube/silicon carbide hybrid materials with high electrical conductivity, superhydrophobicity and superoleophilicity. Carbon 80:120–126
17. Liu Y, Hu C, Feng W, Men J, Cheng L, Zhang L (2014) Microstructure and properties of diamond/SiC composites prepared by tape-casting and chemical vapor infiltration process. J Eur Ceram Soc 34:3489–3498
18. Wu H, Li Y, Yan Y, Yin J, Liu X, Huang Z, Lee S-H, Jiang D (2014) Processing, microstructures and mechanical properties of aqueous gelcasted and solid-state-sintered porous SiC ceramics. J Eur Ceram Soc 34:3469–3478
19. Srivastava M, Rathee S, Siddiquee AN, Maheshwari S (2018) Investigation on the effects of silicon carbide and cooling medium during multi-pass FSP of Al-mg/SiC surface composites. Silicon:1–9
20. Zerfaoui H, Dib D, Kadem B (2018) The simulated effects of different light intensities on the SiC-based solar cells. Silicon:1–7
21. Haibo O, Jianfeng H, Xierong Z, Liyun C, Cuiyan L, Xinbo X, Jie F (2014) Visible-light photocatalytic activity of SiC hollow spheres prepared by a vapor–solid reaction of carbon spheres and silicon monoxide. Ceram Int 40:2619–2625
22. Mollicone J, Ansart F, Lenormand P, Duployer B, Tenailleau C, Vicente J (2014) Characterization and functionalization by sol–gel route of SiC foams. J Eur Ceram Soc 34:3479–3487
23. Brunner K, Eberl K, Winter W (1996) Near-band-edge photoluminescence from pseudomorphic Si 1− y C y/Si quantum well structures. Phys Rev Lett 76:303
24. Harame D (2008) SiGe, Ge, and related compounds 3: materials, processing, and devices
25. Demkov AA, Sankey OF (1993) Theoretical investigation of random Si-C alloys. Phys Rev B 48:2207
26. Becke AD, Johnson ER (2006) A simple effective potential for exchange, ed: AIP
27. Tran F, Blaha P, Schwarz K (2007) Band gap calculations with Becke–Johnson exchange potential. J Phys Condens Matter 19: 196208
28. Tran F, Blaha P (2009) Accurate band gaps of semiconductors and insulators with a semilocal exchange-correlation potential. Phys Rev Lett 102:226401
29. Koller D, Tran F, Blaha P (2012) Improving the modified Becke-Johnson exchange potential. Phys Rev B 85:155109
30. Friedel J (1955) LX. Deviations from Vegard's law. The London, Edinburgh, and Dublin Philosophical Magazine and Journal of Science 46:514–516
31. L. Vegard, "Die konstitution der mischkristalle und die raumfüllung der atome," *Zeitschrift für Physik A Hadrons and Nuclei*, vol. 5, pp. 17-26, 1921.
32. Kasper E, Schuh A, Bauer G, Holländer B, Kibbel H (1995) Test of Vegard's law in thin epitaxial SiGe layers. J Cryst Growth 157:68–72
33. Jacob K, Raj S, Rannesh L (2007) Vegard's law: a fundamental relation or an approximation? Int J Mater Res 98:776–779
34. Singh DJ (1994) Introduction to the LAPW method. Planewaves, pseudopotentials and the LAPW method. Springer, pp 35–43
35. Blaha P, Schwarz K, Madsen G, Kvasnicka D, Luitz J (2001) wien2k. An augmented plane wave+ local orbitals program for calculating crystal properties
36. J. P. Perdew, "JP Perdew and Y. Wang, Phys. Rev. B 45, 13244 (1992), Accurate and simple analytic representation of the electron-gas correlation energy
37. Kohn W, Sham LJ (1965) Self-consistent equations including exchange and correlation effects. Phys Rev 140:A1133
38. Hohenberg P, Kohn W (1964) Inhomogeneous electron gas. Phys Rev 136:B864
39. Broughton J, Bagus P (1989) 14 computer modelling of semiconductor interfaces. Chemistry of the semiconductor industry, p 306
40. Shur MS (1996) Handbook series on semiconductor parameters, vol 1. World Scientific
41. Adams GB, O'Keeffe M, Demkov AA, Sankey OF, Huang Y-M (1994) Wide-band-gap Si in open fourfold-coordinated clathrate structures. Phys Rev B 49:8048–8053
42. Koller D, Tran F, Blaha P (2011) Merits and limits of the modified Becke-Johnson exchange potential. Phys Rev B 83:195134
43. Iyer S, Eberl K, Goorsky M, Tsang J, LeGoues F, Cardone F, Ek B (1992) Si1-y C y Alloys—extending Si-based Heterostructure engineering," in *Amorphous and Crystalline Silicon Carbide IV*, ed: Springer, pp. 13–22
44. Camargo-Martínez J, Baquero R (195106, 2012) Performance of the modified Becke-Johnson potential for semiconductors. Phys Rev B 86
45. Van Vechten J, Bergstresser T (1970) Electronic structures of semiconductor alloys. Phys Rev B 1:3351
46. Jobst B, Hommel D, Lunz U, Gerhard T, Landwehr G (1996) E0 band-gap energy and lattice constant of ternary Zn1− xMgxSe as functions of composition. Appl Phys Lett 69:97–99
47. Zollner S, Vartanian V, Liu J, Zaumseil P, Osten H, Demkov A, Nguyen B-Y (2006) Optical Properties, Elasto-Optical Effects, and Critical-point parameters of Biaxially stressed Si 1-y C y Alloys on Si. SiGe technology and device meeting, 2006. ISTDM 2006. Third international, pp 1–2
48. Bernard JE, Zunger A (1987) Electronic structure of ZnS, ZnSe, ZnTe, and their pseudobinary alloys. Phys Rev B 36:3199
49. Ohfuti M, Sugiyama Y, Awano Y, Yokoyama N (2001) Electronic structure of Si 1− y C y and Si 1− x− y Ge x C y alloys with low C concentrations. Phys Rev B 63:195202
50. Otero-de-la-Roza A, Luaña V (2011) Gibbs2: a new version of the quasi-harmonic model code. I. Robust treatment of the static data. Comput Phys Commun 182:1708–1720
51. Blanco M, Francisco E, Luana V (2004) GIBBS: isothermal-isobaric thermodynamics of solids from energy curves using a quasi-harmonic Debye model. Comput Phys Commun 158:57–72
52. Flórez M, Recio J, Francisco E, Blanco M, Pendás AM (2002) First-principles study of the rocksalt–cesium chloride relative phase stability in alkali halides. Phys Rev B 66:144112
53. Poirier J-P (2000) Introduction to the physics of the Earth's interior. Cambridge University Press
54. Francisco E, Blanco M, Sanjurjo G (2001) Atomistic simulation of Sr F 2 polymorphs. Phys Rev B 63:094107
55. Blanco M Á (1997) Métodos cuánticos locales para la simulación de materiales iónicos: fundamentos, algoritmos y aplicaciones
56. Flubacher P, Leadbetter A, Morrison J (1959) The heat capacity of pure silicon and germanium and properties of their vibrational frequency spectra. Philos Mag 4:273–294
57. Clark C (1964) CD Clark, PJ Dean, and PV Harris, Proc. Roy. Soc.(London) A277, 312 in Proc. Roy. Soc.(London), 1964, p. 312